JOURNAL OF PROPULSION AND POWER
Vol. 17, No. 3, May–June 2001

Pressure Drop Across a Double-Outlet Vortex Chamber

Georgios H. Vatistas* and Peter Sakaris†
Concordia University, Montreal, Quebec H3G 1M8, Canada

The properties of the pressure drop in a medium-aspect-ratio vortex chamber with double outlets are examined both experimentally and theoretically. Dimensional analysis provides the functional relationships between the main dimensionless groups. Application of the integral equations of continuity and energy over the control volume, along with the minimum-pressure-drop principle, furnish the required formulas that relate the predominant nondimensional parameters. In the vortex-dominated regime, the theoretical results, given in terms of the pressure drop across the chamber, are found to agree with the experimental observations. The larger outlet has been shown to control the flow. A considerable reduction in static pressure drop across the chamber can be gained by adding an extra outlet at the opposite end-plate.

Nomenclature

A_{in}	=	total inlet area
A_0	=	cross-sectional area of the vortex chamber, πR_0^2
P	=	static pressure
P_a	=	ambient static pressure
P_{in}	=	static pressure at the inlet
P_{out}	=	static pressure at the outlet
Q_e	=	volumetric flowrate through exit e
Q_{in}	=	inlet volumetric flow rate
Q_u	=	volumetric flowrate through exit u
$\boldsymbol{q}_{\text{in}}$	=	total velocity vector at the inlet
R_{ce}	=	core radius at exit e
R_{cu}	=	core radius at exit u
R_e	=	radius of exit e
R_u	=	radius of exit u
R_0	=	radius of the chamber
r, θ, z	=	radial, tangential, and axial coordinates, respectively
V_r, V_θ, V_z	=	radial, tangential, and axial velocity components
V_{ze}	=	axial velocity component at exit e
V_{zu}	=	axial velocity component at exit u
$V_{\theta\,\text{in}}$	=	inlet tangential velocity component
β_e	=	swirl parameter based on exit e, $\{(A_{\text{in}}/A_0)/[R_e/R_0\cos(\varphi)]\}^2$
β_u	=	swirl parameter based on exit u, $\{(A_{\text{in}}/A_0)/[R_u/R_0\cos(\varphi)]\}^2$
Γ_{in}	=	vortex strength at the inlet $2\pi R_0 V_{\theta\,\text{in}}$
ΔP	=	static pressure difference, $P_{\text{in}} - P_a$
ΔP_e	=	static pressure difference, $(P_{\text{in}} - P_a)_e$
ΔP_u	=	static pressure difference, $(P_{\text{in}} - P_a)_u$
δ_e	=	fraction of the volumetric flow rate trough exit eQ_e/Q_{in}
δ_u	=	fraction of the volumetric flow rate trough exit uQ_u/Q_{in}
λ	=	square of the diameter ratio of the exits, $(R_u/R_e)^2$
ρ	=	density of the fluid
φ	=	angle between the total velocity vector and the tangential velocity component at the inlet (inlet angle)
χ_{ce}	=	dimensionless core size at exit e, R_{ce}/R_e
χ_{cu}	=	dimensionless core size at exit u, R_{cu}/Ru

Received 15 March 2000; revision received 20 October 2000; accepted for publication 29 October 2000.

*Professor, Mechanical Engineering Department, 1455 DeMaisonneuve Boulevard West. Senior Member AIAA.

†Research Assistant, Mechanical Engineering Department, 1455 DeMaisonneuve Boulevard West.

I. Introduction

THE behavior of concentrated vortices confined in cylindrical tubes and their interaction with the host flowfield is important for three main reasons. First, swirl can be found in many engineering applications. In some, the presence of the vortex is an essential element for the proper operation of the equipment, and the designer tries to produce it efficiently. In others, swirl is a parasitic flow manifestation superimposed on the main fluid motion. Its presence reduces the efficiency of the equipment and produces vibrations and noise, and the designer strives to suppress it. Second, important phenomena such as vortex breakdown and the main characteristics of high Rossby number geophysical vortices may be reproduced in tubes and then analyzed under controlled laboratory conditions. Third, the general area is also of interest to ion flow dynamics, low-temperature physics, geophysics, and to several other related fields.

The favorable properties of swirling flows confined in tubes have been employed in many engineering systems. The vortex separator is one of the most widespread and probably the oldest of the industrial applications.[1] Energy separation may be achieved in vortex tubes.[2–4] The vortex pump takes advantage of the vacuum conditions developed inside the core and is used to pump liquids.[5,6] The experimental work on double-outlet vortex chambers had as motivation the improvement of collection efficiency in hydraulic cyclones. The work of Dahlstrom[7] dealt mainly with the flow distribution and the pressure drop in a water–plastic sphere system, whereas Kelsall[8,9] used a water–quartz fines. Rietema[10] investigated the same flow properties using a water–glycerol mixture. In addition to the hydraulic cyclone, the dust separator, the vortex pump, the Ranque–Hilsch tube, and others utilize a doublet-outlet arrangement. Despite the extensive technical literature on vortex chamber flows, the paucity of any substantial analytical work dealing with the flow in a double-outlet chamber was surprising.

One of the most important operational characteristics in vortex chambers is the pressure drop. This has been the subject of several studies in the past.[11–16] However, previous work has focused on vortex chambers with a single outlet placed at the top or on the bottom plates. The work to be presented here deals with the main flow properties in chambers having two axial outlet ports. Based on dimensional analysis, the functional relationships of the main dimensionless groups will be given. The analytical work, which is an extension of previous work by Vatistas et al.,[15,16] in single-outlet chambers, provides the formulas that relate the dominant nondimensional parameters. For strongly swirling flows with small inlet angle, the experimental results will be shown to agree reasonably well with the theoretical findings.

II. Experimental Facility

Vortex chambers in general have a cylindrical configuration with a centrally placed outlet(s) located at the top, the bottom plate, or on

both plates. Fluid entering the tube acquires swirl via either 1) inlets placed tangentially around the wall, 2) rotation of a porous wall, or 3) admission through radial or axial vanes. The inlet(s) may be located near the top plate, the opposite end, both, in the middle, or cover the entire length of the chamber. Both inlet(s) with rectangular or circular cross section(s) have been used in the past. The present experiments have been conducted using a jet-driven vortex chamber similar to the one utilized by Vatistas et al.[16] The main difference between the two is that in the latest version, shown schematically in Fig. 1, an arrangement has been made such that two exits instead of one may be incorporated. The swirl generator, which can be placed at any intermediate position between the two endplates, offers a wider flexibility in the selection of the inlet conditions. Its modular design makes the variation of the area ratio (A_{in}/A_0) and the inlet flow angle φ easier. The required set of inlet conditions are realized by insertion of the appropriate vortex generator blocks (swirlers) into the vortex generator assembly. Along the periphery of the vortex generator block, a number of openings of a circular cross section are drilled at a specified angle φ. The static pressure is measured by a series of taps located ahead of the tangential ports, and it is averaged by connecting in parallel all of the pressure pickup tubes into a common tube. The values of the pressure were recorded using pressure taps drilled on the cylindrical wall, just above and below the swirl generator. The measurements of the mean gauge pressure, $P_{in} - P_a$, were obtained using a well type inclined manometer filled with Meriam 100 unity oil, with a specific gravity equal to 0.787. The manometer can be adjusted to several inclined positions, which gives an uncertainty of $\pm 1.27 \times 10^{-4}$ m of H_2O (lowest) and $\pm 2.54 \times 10^{-3}$ m of H_2O (vertical) positions. A rotameter was used to measure the volumetric flow rate of the inlet air and has been calibrated at standard pressure and temperature conditions.

The geometrical characteristics of the vortex chamber used for the present experiments are given in Table 1. The chamber has a cylindrical shape with constant cross-sectional area. Its length, defined as the distance between the two endplates, was kept constant. The axis of the vortex chamber was horizontal with respect to the ground, with the swirler placed in the middle. The design of the swirler was made in a way that the total inlet area did not change with the inlet angle φ. Air at standard temperature was the working fluid. A typical experimental run involved the following simple routine. A specific size e outlet was fixed onto the two ends of the chamber. The flow rate was set at $Q_{in} = 1.89 \times 10^4$ cm^3/s (this value was used for all of the tests). The static pressure was recorded using the manometers mentioned earlier. The size of the u outlet was then changed, and the process was then repeated. In every test run, the size of the e outlet was kept constant while the u outlet varied.

Table 1 Geometrical characteristics of the vortex chamber[a]

φ, deg	A_{in}, cm^2	Exit orifice radius, cm	Total length, cm
20	29.03	1.40, 0.94, 0.79, 0.71	39.370
30	27.25	——	——
40	——	——	——
60	——	——	——

[a] $D = 14$ cm.

III. Analysis

It has been shown previously[16] that, when the centrifugal forces dominate the flow, the nondimensional core size (radius of maximum tangential velocity) and static pressure drop across a single-outlet vortex chamber are given, respectively, by

$$\chi_{ce} = f_n(\beta_e)$$

and

$$\left(2\Delta P \Big/ \rho q_{in}^2 + 1\right)(R_e/R_0)^2/\cos^2(\varphi) = f_n(\chi_{ce})$$

where $\chi_{ce} = R_{ce}/R_e$, and

$$\beta_e = \left[\frac{A_{in}/A_0}{R_e/R_0\cos(\varphi)}\right]^2$$

Consider now the flow inside the double-outlet vortex chamber shown in Fig. 1. In the case where two outlets are involved, the functional relationships of the main parameters are assumed to be given by

$$R_{cu} = f_n(\Gamma_{in}, Q_{in}, R_u), \qquad R_{ce} = f_n(\Gamma_{in}, Q_{in}, R_e)$$

$$\Delta P_u = f_n(\Gamma_{in}, R_u, R_{cu}), \qquad \Delta P_e = f_n(\Gamma_{in}, R_e, R_{ce})$$

From continuity,

$$\delta_e + \delta_u = 1$$

where $\delta_e = Q_e/Q_{in}$ and $\delta_u = Q_u/Q_{in}$. Dimensional analysis gives, respectively,

$$\chi_{cu} = f_n[(1-\delta_e)\beta_u] \tag{1}$$

$$\chi_{ce} = f_n(\delta_e\beta_e) \tag{2}$$

$$\left(2\Delta P_u \Big/ \rho q_{in}^2 + 1\right)(R_u/R_0)^2 \Big/ \cos^2(\varphi) = f_n(\chi_{cu}) \tag{3}$$

$$\left(2\Delta P_e \Big/ \rho q_{in}^2 + 1\right)(R_e/R_0)^2 \Big/ \cos^2(\varphi) = f_n(\chi_{ce}) \tag{4}$$

where $\lambda = (R_u/R_e)^2$, $\chi_{cu} = R_{cu}/R_u$, and

$$\beta_u = \left(\frac{A_{in}/A_0}{R_u/R_0\cos(\varphi)}\right)^2$$

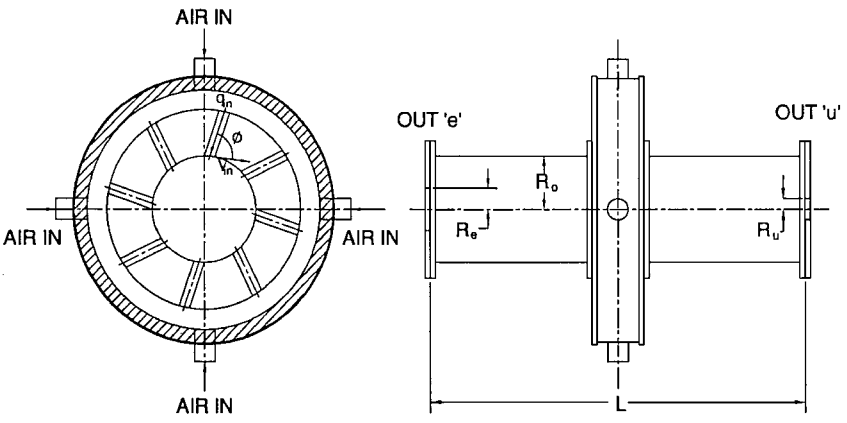

Fig. 1 Schematic of the vortex chamber.

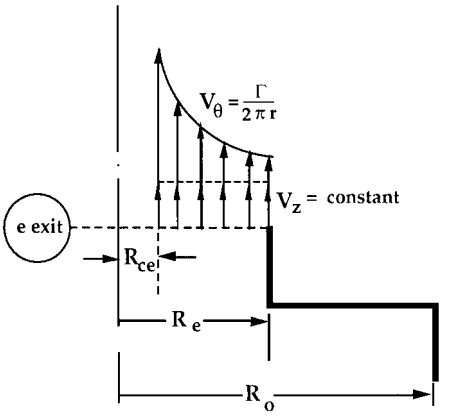

Fig. 2 Assumed exit conditions.

The swirl parameter β is the reciprocal square root of the swirl number (defined as the square of the ratio of the angular to axial momenta) often quoted in the technical literature. Realization that

$$\Delta P_u = \Delta P_e$$

leads to the relationship

$$\lambda^2 f_n(\delta_e \beta_e) - f_n[(1-\delta_e)\beta_u] = 0 \tag{5a}$$

or in functional form,

$$\delta_e = f_n(\lambda, \beta_e) \tag{5b}$$

The preceding analysis furnishes the expected functional relations among the main dimensionless parameters associated with the problem. Based on the energy and continuity equations and the minimum-pressure principle, formulas relating these parameters will be presented. To simplify the problem, several assumptions (as was the case with the flow in a single-outlet chamber) are also employed here. These are 1) the pressure and the total velocity at the inlet are both uniform and 2) the radial velocity component on both exits is neglected, the axial component is constant and extends as far as the core size, and the tangential component has a hyperbolic profile (see Fig. 2).

Energy balance over the control volume enclosing the chamber, assuming that at both exits the pressure is ambient and neglecting viscous effects, yields

$$\left(\frac{P_{\text{in}}}{\rho} + \frac{1}{2}q_{\text{in}}^2\right) Q_{\text{in}} = \int_{R_{cu}}^{R_u} \left\{ \frac{P_a}{\rho} + \frac{1}{2}\left[\left(\frac{\Gamma_{\text{in}}}{2\pi r} \right)^2 + V_{zu}^2 \right] \right\} V_{zu} 2\pi r \, \mathrm{d}r$$

$$+ \int_{R_{ce}}^{R_e} \left\{ \frac{P_a}{\rho} + \frac{1}{2}\left[\left(\frac{\Gamma_{\text{in}}}{2\pi r} \right)^2 + V_{ze}^2 \right] \right\} V_{ze} 2\pi r \, \mathrm{d}r \tag{6}$$

Performing the integration, followed by simplification of the results using continuity, and furthermore noting that

$$V_{zu} = \frac{Q_{\text{in}}\delta_u}{\pi\left(R_u^2 - R_{cu}^2\right)} \qquad V_{ze} = \frac{Q_{\text{in}}\delta_e}{\pi\left(R_e^2 - R_{ce}^2\right)}$$

Eq. (6) becomes

$$\overline{\Delta P} = \left(\frac{2\Delta P}{\rho q_{\text{in}}^2} + 1 \right) \frac{(R_e/R_0)^2}{\cos^2(\varphi)} = \left[\frac{\delta_u^2 \beta_u}{\left(1-\chi_{ce}^2\right)^2} - \frac{2\,\ell n(\chi_{cu})}{\left(1-\chi_{cu}^2\right)} \right] \frac{\delta_u}{\lambda}$$

$$+ \left[\frac{\delta_e^2 \beta_e}{\left(1-\chi_{ce}^2\right)^2} - \frac{2\,\ell n(\chi_{ce})}{\left(1-\chi_{ce}^2\right)} \right] \delta_e \tag{7}$$

where $\Delta P = P_{\text{in}} - P_a$.

A careful study of Eq. (7) reveals that

$$\lim_{\chi_{cu}\to 0} \left(\overline{\Delta P}\right) = \lim_{\chi_{ce}\to 0} \left(\overline{\Delta P}\right) = \infty$$

and

$$\lim_{\chi_{cu}\to 1} \left(\overline{\Delta P}\right) = \lim_{\chi_{ce}\to 1} \left(\overline{\Delta P}\right) = \infty$$

The described behavior of the pressure drop is attributed to that, as χ_{ce} and χ_{cu} both tend to zero, the tangential velocity component at the exit goes asymptotically to infinity. On the other hand, when χ_{ce} and χ_{cu} both go toward one, and to satisfy continuity, the exit axial velocity component tends to infinity. There must exist $0 < \chi_{cu} < 1$ and $0 < \chi_{ce} < 1$ such that $\overline{\Delta P}$ is minimum. The latter requires the following conditions.

Condition 1:

$$\frac{\partial \overline{\Delta P}}{\partial \chi_{cu}} = 0$$

Condition 2:

$$\frac{\partial \overline{\Delta P}}{\partial \chi_{ce}} = 0$$

Operation of conditions 1 and 2 on Eq. (7) yields,

$$\chi_{cu}^4[2\,\ell n(\chi_{cu}) - 1] + 2\chi_{cu}^2\left[1 + (1-\delta_e)^2\beta_u - \ell n(\chi_{cu})\right] - 1 = 0 \tag{8}$$

and

$$\chi_{ce}^4[2\,\ell n(\chi_{ce}) - 1] + 2\chi_{ce}^2\left[1 + \delta_e^2\beta_e - \ell n(\chi_{ce})\right] - 1 = 0 \tag{9}$$

respectively, where $\beta_e = \lambda\beta_u$.

There are two equations available, that is, Eqs. (8) and (9), and there are three unknowns, χ_{ce}, χ_{cu}, and δ_e. The necessary third equation to close the system comes from the comparability of the pressure:

$$\overline{\Delta P} = \lambda \overline{\Delta P}_e \tag{10a}$$

and

$$\overline{\Delta P} = \overline{\Delta P}_u \tag{10b}$$

where

$$\overline{\Delta P}_u = \left\{ \frac{2\Delta P_u}{\rho q_{\text{in}}^2} + 1 \right\} \frac{(R_u/R_0)^2}{\cos^2(\varphi)} = \frac{\delta_u^2 \beta_u}{\left(1-\chi_{cu}^2\right)^2} - \frac{2\,\ell n(\chi_{cu})}{\left(1-\chi_{cu}^2\right)} \tag{10c}$$

and

$$\overline{\Delta P}_e = \left\{ \frac{2\Delta P_e}{\rho q_{\text{in}}^2} + 1 \right\} \frac{(R_e/R_0)^2}{\cos^2(\varphi)} = \frac{\delta_e^2 \beta_e}{\left(1-\chi_{ce}^2\right)^2} - \frac{2\,\ell n(\chi_{ce})}{\left(1-\chi_{ce}^2\right)} \tag{10d}$$

Equations (10a) and (10b) also imply that

$$\overline{\Delta P}_u = \lambda \overline{\Delta P}_e \tag{10}$$

Substitution of $\overline{\Delta P}_u$ and $\overline{\Delta P}_e$ in Eq. (10) and multiplication through by $(1-\chi_{ce}^2)^2(1-\chi_{cu}^2)^2$, followed by simplifications and collection of terms give

$$b_1\delta_e^2 + b_2\delta_e + b_3 = 0 \tag{11}$$

where

$$b_1 = 1 - \lambda^2 \frac{\left(1-\chi_{cu}^2\right)^2}{\left(1-\chi_{ce}^2\right)^2} \qquad b_2 = -2$$

and

$$b_3 = \frac{2\lambda}{\beta_e}\left(1-\chi_{cu}^2\right)\left\{ \lambda \frac{\left(1-\chi_{cu}^2\right)}{\left(1-\chi_{ce}^2\right)} \ell n(\chi_{ce}) - \ell n(\chi_{cu}) \right\} + 1$$

The solution to the system of Eqs. (8), (9), and (11) is obtained using the following procedure:

1) Assume a value of δ_e $(0 < \delta_e < 1)$.

2) Calculate the roots of χ_{ce}, and χ_{cu} to the desired precision from Eqs. (8) and (9), respectively, via a root-finding numerical method.

3) Obtain from Eq. (11) the value of δ_e using the quadratic formula.

4) Is δ_e calculated sufficiently close to the assumed value? If it is not, go to step 2. If the answer is yes, then the solution has been reached, and the remaining properties can now be calculated.

Knowing the values of χ_{ce}, χ_{cu}, and δ_e the pressure drop can then be calculated. From Eq. (9) we have

$$\delta_e^2\beta_e - 2\left(1-\chi_{ce}^2\right)\ln\left(\chi_{ce}^2\right) = \left\{\left(1-\chi_{ce}^2\right)\left[\left(1-\chi_{ce}^2\right) - 2\chi_{ce}^2\ln(\chi_{ce})\right]\right\}\Big/ 2\chi_{ce}^2 \tag{12}$$

Rearranging Eq. (10d) yields

$$\overline{\Delta P}_e = \left[\delta_e^2\beta_e - 2\left(1-\chi_{ce}^2\right)\ln(\chi_{ce})\right]\Big/\left(1-\chi_{ce}^2\right)^2 \tag{13}$$

Inserting Eq. (12) into (13) gives, after some obvious simplifications,

$$\overline{\Delta P}_e = \frac{1-\chi_{ce}^2[1+2\ln(\chi_{ce})]}{2\chi_{ce}^2\left(1-\chi_{ce}^2\right)} \tag{14}$$

The preceding equation provides the pressure drop across exit e as a function of χ_{ce} alone.

IV. Discussion of the Results

A typical variation of the two core sizes as a function of the diameter ratio λ is given in Fig. 3. For $\lambda = 1$, a reduction of the outlet diameter of the u exit, keeping β_e constant, will result in a contraction of the core size at the e exit. For $\lambda > 1$, increasing λ results in a decrease of χ_{cu}, while χ_{ce} becomes larger.

Figure 4 shows the qualitative properties of flow rate distribution when R_u varies while R_e remains constant. Two special cases are worth noting. The first case, $\lambda \to 0$, may be represented by the flow situation where $R_e = \text{const}$, while $R_u \to 0$. For this condition, $\delta_u \to 0$. Equation (8) simplifies to

$$\chi_{cu}^4[2\ln(\chi_{cu}) - 1] + 2\chi_{cu}^2[1 - \ln(\chi_{cu})] - 1 = 0$$

This equation has only one positive root, which it is located at $\chi_{cu} = 1$. Under this condition, b_1 and $b_3 \to 1$, and Eq. (11) points out that $\delta_e \to 1$, while for continuity, $\delta_u \to 0$. In the other side of λ, that is, for $\lambda > 1$, the distribution of flow rates between the two outlets exhibits the opposite behavior.

The second case, $\lambda \to 1$, represents the symmetric flow where the outlets are of the same size and, thus, $\beta_e = \beta_u$. This suggests that χ_{ce} must be equal to χ_{cu}. If $\chi_{ce} = \chi_{cu}$, then Eq. (11) becomes

$$2\delta_e - b_3 = 0$$

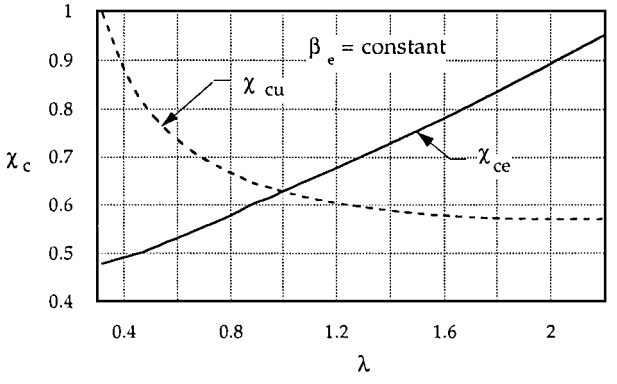

Fig. 3 Typical variation of the core size with λ.

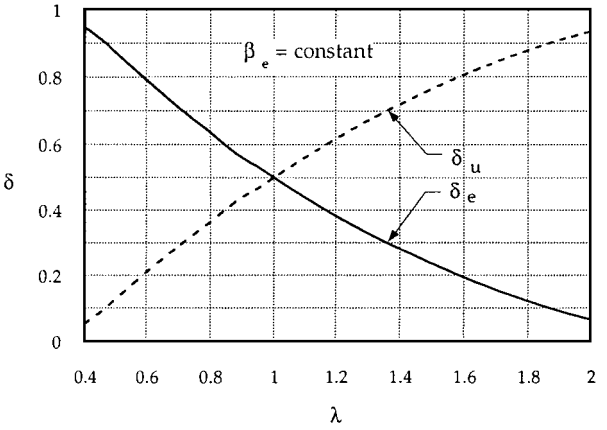

Fig. 4 Typical flow distribution as a function of λ.

indicating that $\delta_e = 0.5$, and, therefore, $\delta_u = 0.5$, or that the flow is equally distributed between the two exits. The last results makes Eqs. (8) and (9) symmetric, and by induction, the conjecture is validated.

The behavior of the pressure drop across the vortex chamber (based on e) is shown in Figs. 5a–5d. Comparisons of the experimentally obtained $\overline{\Delta P}_e$ with the theory are given in Figs. 5. For small inlet angles (Figs. 5a–5c), the agreement between the two is seen to be excellent. This is to be expected because the analysis is based on the assumption that the centrifugal effects dominate. For a larger φ (see Fig. 5d), where the basic assumption is not met, the agreement between the two deteriorates. From Figs. 5a–5c, we see that for $\lambda < 1$, exit e, which is the larger outlet, controls the pressure, whereas for $\lambda > 1$, the control is transferred to the u outlet. Also see Fig. 6 for pressure drop based on e and u outlets.

All of the mentioned graphs indicate that as parameter $\lambda \to 0$, which in turn implies that R_u decreases (while R_e remains constant), pressure $\overline{\Delta P}_e$ asymptotically approaches the value of a single-outlet chamber given by Vatistas et al.[3] (see Fig. 6, Ref. 3). In this case, from Eq. (10), $\overline{\Delta P}_u \to 0$.

It is important to further explore the circumstances where $\lambda = 1$, or when the flow is symmetric, which implies that $\chi_{ce} = \chi_{cu}$ and $\overline{\Delta P}_e = \overline{\Delta P}_u$. Consider the event where we have two chambers, one having a single outlet and the other two outlets. Assume that the geometric and flow parameters in both chambers are the same. In this case, the single- to double-outlet pressure drop is

$$\Delta\Pi = \left\{\frac{2\Delta P_{ed}}{\rho q_{\text{in}}^2} + 1\right\}\Big/\left\{\frac{2\Delta P_{es}}{\rho q_{\text{in}}^2} + 1\right\} = \left[\frac{1-\chi_{ces}^2}{1-\chi_{ced}^2}\right]^2 \frac{\beta_{ed} - 8\left(1-\chi_{ced}^2\right)\ln(\chi_{ced})}{\beta_{es} - 2\left(1-\chi_{ces}^2\right)\ln(\chi_{ces})} \tag{15}$$

The results of Eq. (15), shown in Fig. 7, hint that a considerable reduction in static pressure drop across the chamber can be achieved through the incorporation of two instead of one outlet. The degree of pressure reduction is also seen to increase with parameter β_e. Because the development of the tangential velocity component inside the chamber depends principally on the inlet and outlet geometric parameters, the incorporation of the second flow exit will not affect the centrifugal force field in any fundamental way.

All of the given results were obtained with the swirler located midway of the chamber. The position of the swirler was originally expected to influence the development of the flow component in the r–z plane. However, experiments have shown conclusively that the pressure drop is not a strong function of the location of the swirler. Hence, the results apply irrespective of the swirler's location. The latter finding is consistent with the assumption that the swirling component of the flow dominates the one taking place in the r–z plane.

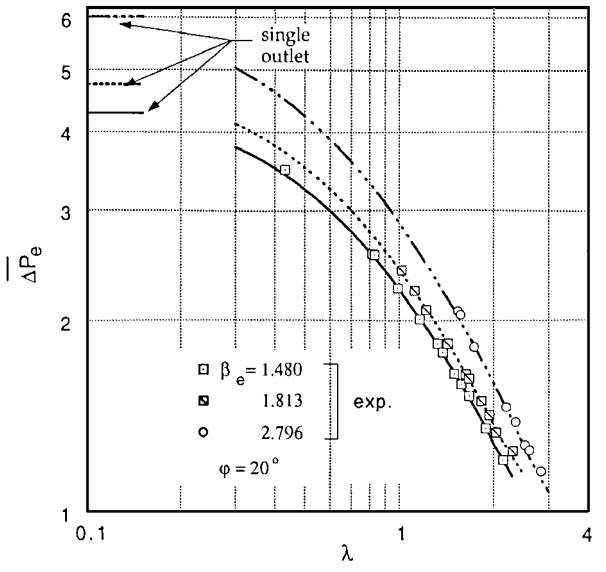

a) $\varphi = 20$ deg

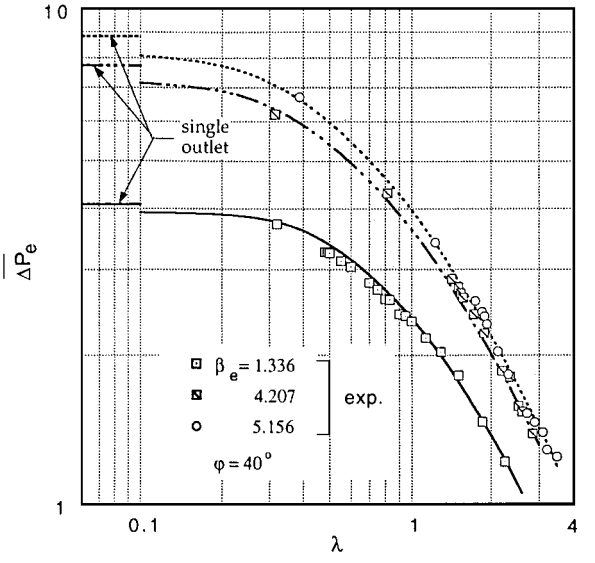

c) $\varphi = 40$ deg

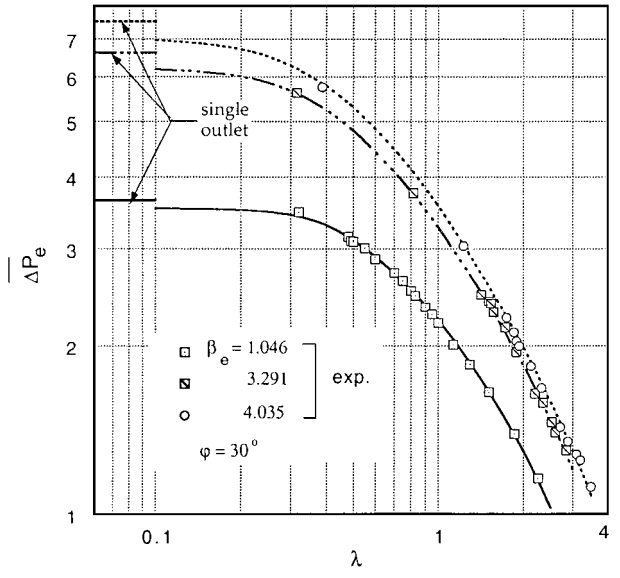

b) $\varphi = 30$ deg

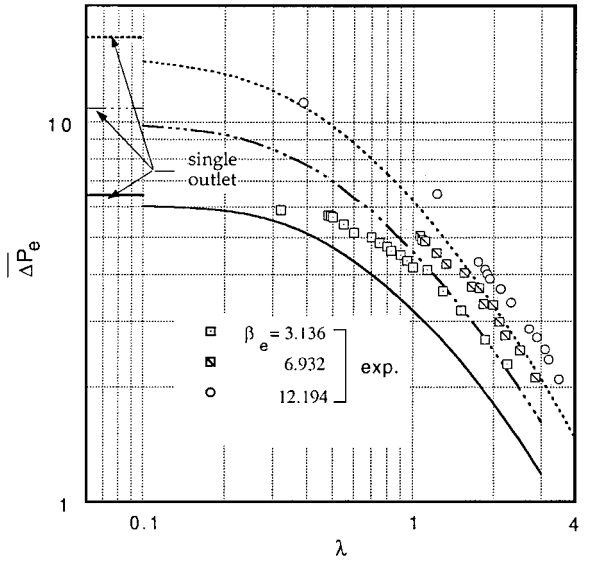

d) $\varphi = 60$ deg

Fig. 5 Experimental and calculated values of the pressure drop across the chamber as a function of λ (curves represent results obtained from the present theory).

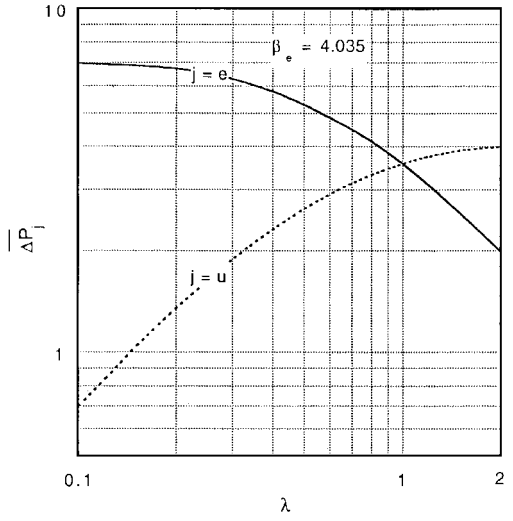

Fig. 6 Pressure drop based on *e* and *u* outlets, as a function of diameter ratio number λ ($\beta_e = 4.035$).

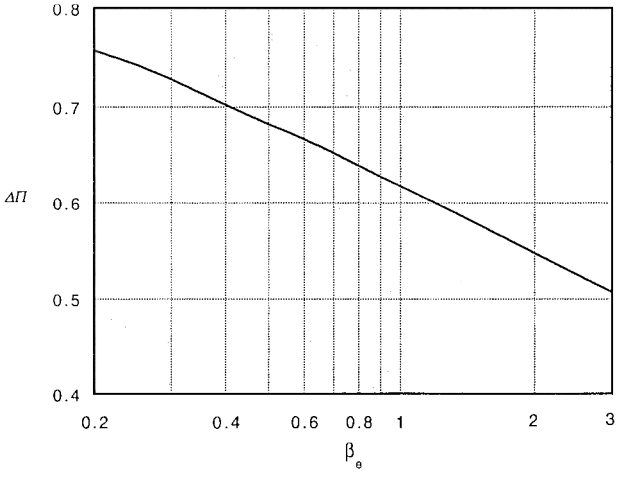

Fig. 7 Pressure drop ratio between single- and double-outlet vortex chambers as a function of the controlling swirl number β_e.

V. Conclusions

The present paper has examined the static pressure drop across a vortex chamber with multiple outlets. In the vortex-dominated region, the theoretical results, given in terms of the pressure drop across the chamber, were found to be consistent with the observations. As the size of one of the exits decreased, while the other remained constant, the pressure drop was seen to approach the value of a single-outlet chamber. The experiments revealed that the location of the swirler does not significantly affect the pressure drop across the chamber. The theory suggests that the flow is controlled by the larger diameter exit. It was also shown that a considerable reduction in static pressure drop across the chamber may be achieved by adding an extra outlet (of the same size) to a single exit chamber. Although in the present theory the ambient pressure at both exits was assumed to be the same, other conditions may be easily accommodated by a simple modification to the present theory.

References

[1]Gupta, A. K., Lilley, D. G., and Syred, N., *Swirl Flows*, Abacus, Tunbridge Wells, England, U.K., 1984.

[2]Ranque, G., "Expériences sur la Détente Gigatoire avec Productions Simultanées d'un Echappement d'Air Chaud et d'un Echappement d'Air Froid," *Journal de Physique et le Radium*, Vol. 4, No. 7, 1933, pp. 1123–1158.

[3]Hilsch, R., "The Use of the Expansion of Gases in a Centrifugal Field," *Zeitshrift fuer Naturforschung*, Vol. 1, 1946, pp. 208–214, *Review of Scientific Instruments*, Vol. 18, No. 2, 1947, pp. 108–113 (translation).

[4]Deissler, R. G., and Perlmutter, M., "Analysis of the Flow and Energy Separation in a Turbulent Vortex," *International Journal of Heat and Mass Transfer*, Vol. 1, No. 2–3, 1960, pp. 173–191.

[5]Schneck, R. J., "The Vortex Ejector Pump," M.E. Thesis, Mechanical Engineering Dept., Concordia Univ., Montreal, 1971.

[6]Struiksma, N., "The Cyclone Pump," *Journal of Hydraulic Research*, Vol. 23, No. 2, 1985, pp. 165–178.

[7]Dahlstrom, D. A., "Cyclone Operating Factors and Capacities on Coal and Refuse Slurries," *Transactions of AIME*, Vol. 184, Sept. 1949, pp. 331–344.

[8]Kelsall, D .F., "A Study of the Motion of Solid Particles in a Hydraulic Cyclone," *Transactions. Institution of Chemical Engineers*, Vol. 30, No. 2, 1952, pp. 87–108.

[9]Kelsall, D. F., "A Further Study of the Hydraulic Cyclone," *Chemical Engineering Science*, Vol. 2, 1953, pp. 254–272.

[10]Rietema, K., "Performance and Design of Hydrocyclones-I, II and III," *Chemical Engineering Science*, Vol. 15, Nos. 3 and 4, 1961, pp. 298–315.

[11]Troyankin, Y .U., and Baluev, E. D., "The Aerodynamic Resistance and Efficiency of Cyclone Chamber," *Thermal Engineering*, Vol. 16, 1969, pp. 45–50.

[12]Tager, S. A., "Calculating the Aerodynamic Resistance of Cyclone Combustion Chamber," *Thermal Engineering*, Vol. 18, No. 7, 1971, pp. 88–91.

[13]Lewellen, W. S., "A Review of Confined Vortex Flows," NASA CR-1772, July 1971.

[14]Shakespeare, W. J., and Levy, E. K., "Pressure Drop in a Confined Vortex with High Flow Rate," American Society of Mechanical Engineers, Winter Annual Meeting, Nov. 1980.

[15]Vatistas, G. H., Lin, S., and Kwok, C. K., "Theoretical and Experimental Studies on Vortex Chamber Flows," *AIAA Journal*, Vol. 24, No. 4, 1986, pp. 635–642.

[16]Vatistas, G. H., Lam, C., and Lin, S., "A Similarity Relationship for the Pressure Drop in Vortex Chambers," *Canadian Journal of Chemical Engineering*, Vol. 67, Aug. 1989, pp. 540–544.